Anal. Bioanal. Electrochem., Vol. 8, No. 7, 2016, 830-847

Analytical & Bioanalytical Electrochemistry

2016 by CEE
www.abechem.com

Full Paper

Poly (1-phenylethene): As a Novel Corrosion Inhibitor for Carbon Steel / Hydrochloric Acid Interface

Khaoula Alaoui,[1] Younes El Kacimi,[1,*] Mouhsine Galai,[1] Khadija Dahmani,[2] Rachid Touir,[1,3] Ahmed El Harfi[4] and Mohamed Ebn Touhami[1]

[1]*Laboratory of Materials Engineering and Environment: Modeling and Application, Faculty of Science, University Ibn Tofail BP. 133-14000, Kenitra, Morocco*
[2]*Laboratory of Materials, Electrochemistry and Environment, Faculty of Science, Ibn Tofail University, Kénitra, Morocco*
[3]*Centre Régional des métiers de l'éducation et de la formation (CRMEF), Avenue Allal Al Fassi, Madinat Al Irfane, BP 6210 Rabat, Morocco*
[4]*Laboratory of Polymers, Radiation and Environment- Team of Macromolecular & Organic Chemistry, Faculty of Science, University Ibn Tofail, Kenitra, Morocco*

*Corresponding Author, Tel.: +212 6 63 56 65 45
E-Mail: elkacimiyounes@yahoo.fr

Received: 17 May 2016 / Received in revised form: 16 September 2016 / Accepted: 24 September 2016 / Published online: 15 November 2016

Abstract- In this paper, the inhibition ability of *Poly(1-phenylethene)* against the carbon steel corrosion in 1.0 M HCl solution was studied at different temperatures range from 298 to 328 K using weight loss, potentiodynamic polarization and electrochemical impedance spectroscopy (EIS). It was found that the studied compound exhibited a very good performance as inhibitor for carbon steel corrosion in 1.0 M HCl medium. The obtained thermodynamic adsorption parameters (ΔG^*_{ads}, ΔH^*_{ads}, ΔS^*_{ads}) indicated that this polymer retarded both cathodic and anodic processes through physical adsorption and blocking the active corrosion sites. It is found also that this compound obeyed the Langmuir's adsorption isotherm.

Keywords- Corrosion and inhibition, *Poly(1-phenylethene)*, Carbon steel, Hydrochloric acid, Adsorption isotherm, Thermodynamic parameters

1. INTRODUCTION

Carbon steel is among the most widely used engineering materials such as metal-processing equipment, marine applications, nuclear and fossil fuel power plants, transportation, chemical processing, pipelines, mining and construction. Iron and its alloys as construction materials in industrial sectors has become a great challenge for corrosion engineers or scientists nowadays [1]. Acid solutions are commonly used for the removal of undesirable scale and rust in the metal working, cleaning of boilers and heat exchangers. However, over-pickling of metal leads to rough and blistered coating. Formation of protective film on the steel surface and characterization of metal surface is the major subject of interest. In order to reduce the corrosion rate of metals, several techniques has been applied. The use of inhibitors is one of the most practical methods for protection against corrosion in acidic media. Inhibitors, which reduce corrosion on metallic materials, can be divided into three kinds: surfactant inhibitors [2], organic inhibitors [3] and inorganic inhibitors [4]. Heterocyclic inhibitors have many advantages such as high inhibition efficiency [5–8], low price, and easy production. The choice of effective inhibitors was based on their mechanism of action and their electron- donating capability. Moreover, organic molecules could be adsorbed on the metal surface by one of the four following mechanisms: (i) electrostatic interaction between charged surface of metal and the charge of the inhibitor,(ii) interaction of unshared electron pairs in the inhibitor molecule with the metal, (iii) interaction of π-electron with metal and (iv) a combination of the (i) and (iii) types [9-11].

In the others, these compounds can form either a strong coordination bond with metal atom or a passive film on the surface [12]. The corrosion inhibition of a metal may involve either *physisorption* or *chemisorption* of the inhibitor on the metal surface. Electrostatic attraction between the charged hydrophilic groups and the charged active centers on the metal surface leads to *physisorption.* Several authors showed that most inhibitors were adsorbed on the metal surface by displacing water molecules from the surface and forming a compact barrier film [13].

However, the use of polymers as corrosion inhibitors has attracted considerable attention recently. Polymers have been reported as effective corrosion inhibitors because of their high molecular weight and large size they provided high corrosion inhibition [14-19]. Thus, the polymers having large repeating units that may cover more area on the metal surface and formed a metal polymer complex which leads to high inhibition efficiency [20].

In continuation of our work on testing Polyvinyl Alcohol as corrosion inhibitors in acidic media [21], we have studied the inhibition efficiency of poly(1-phenylethene) for carbon steel corrosion in 1.0 M HCl solution using weight loss and electrochemical measurements. The effect of temperature on the corrosion behavior was also studied in the range from 298 to 328 K. The adsorption thermodynamic parameters such as adsorption heat ΔH_a^*, entropy of adsorption ΔS_a^* and adsorption free energy ΔG_a^* were calculated and discussed.

2. EXPERIMENTAL DETAILS

2.1. Weight loss measurements

The chemical composition of the used carbon steel sample is shown in Table 1. The specimen's surface was prepared by polishing with emery paper at different grit sizes (from 180 to 1200), rinsing with distilled water, degreasing with ethanol, and drying at hot air.

Table 1. Chemical composition of the used carbon steel

Material	**Composition, % by wt.**											
	C	**Si**	**Mn**	**Cr**	**Mo**	**Ni**	**Al**	**Cu**	**Co**	**V**	**W**	**Fe**
Carbon steel	0.11	0.24	0.47	0.12	0.02	0.1	0.03	0.14	<0.0012	<0.003	0.06	Balance

The carbon steels specimens used have a rectangular form 2.5 cm×2.0 cm×0.05 cm. The immersion time for weight loss was 6 h at 298 K. After immersion period, the specimens were cleaned according to ASTM G-81 and reweighed to 10^{-4} g for determining corrosion rate [20,21]. The aggressive solution of 1.0 M HCl was prepared by dilution of analytical grade 37% HCl with distilled water. The molecular formula of the examined inhibitor is shown in Figure 1.

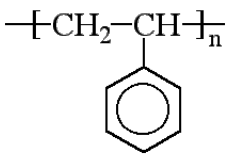

Fig. 1. Chemical structure of poly(1-phenylethene)

However, weight loss allows us to calculate the mean corrosion rate as expressed in mg cm^{-2} h^{-1}.

The inhibition efficiency, η_w%, is determined as follows (Eq. (1)):

$$\eta_\omega\% = \frac{\omega^0_{corr} - \omega_{corr}}{\omega^0_{corr}} \times 100 \quad (1)$$

Where ω^0_{corr} and ω_{corr} are the corrosion rates in the absence and presence of inhibitors, respectively.

2.2. Electrochemical measurements

For electrochemical measurements, the electrolysis cell was a borrosilcate glass (Pyrex®) cylinder closed by a cap with five apertures. Three of them were used for the electrode insertions. The working electrode was pressure-fitted into a polytetrafluoroethylene holder

(PTFE) exposing only 1 cm^2 of area to the solution. Platinum and saturated calomel were used as counter and reference electrode (SCE), respectively. All potentials were measured against the last electrode.

The potentiodynamic polarization curves were recorded by changing the electrode potential automatically from negative values to positive values versus E_{corr} using a Potentiostat/Galvanostat type PGZ 100, at a scan rate of 1 mV s^{-1} after 30 min immersion time until reaching steady state. The test solution was thermostatically controlled at 298 K in air atmosphere without bubbling. To evaluate corrosion kinetic parameters, a fitting by Stern-Geary equation was used. To do so, the overall current density values, *i*, were considered as the sum of two contributions, anodic and cathodic current i_a and i_c, respectively. For the potential domain not too far from the open circuit potential, it may be considered that both processes followed the Tafel law [22]. Thus, it can be derived from Eq. (2):

$$i = i_a + i_c = i_{corr}\left\{\exp\left[b_a \times \left(E - E_{corr}\right)\right] - \exp\left[b_c \times \left(E - E_{corr}\right)\right]\right\} \quad (2)$$

Where i_{corr} is the corrosion current density (A cm^{-2}), b_a and b_c are the Tafel constants of anodic and cathodic reactions (V^{-1}), respectively. These constants are linked to the Tafel slopes β (V/dec) in usual logarithmic scale given by Eq. (3):

$$\beta = \frac{\ln 10}{b} = \frac{2.303}{b} \quad (3)$$

The corrosion parameters were then evaluated by means of nonlinear least square method by applying equation (2) using Origin software. However, for this calculation, the potential range applied was limited to ±0.100V around E_{corr}, else a significant systematic divergence was sometimes observed for both anodic and cathodic branches.

The corrosion inhibition efficiency is evaluated from the corrosion current densities values using the Eq. (4):

$$\eta_{PP} = \frac{i_{corr}^{0} - i_{corr}}{i_{corr}^{0}} \times 100 \quad (4)$$

The surface coverage values (θ) have been obtained from polarization curves for various concentrations of inhibitor using the Eq. (5) [23]:

$$\theta = 1 - \frac{i_{corr}}{i_{corr}^{0}} \quad (5)$$

Where i_{corr}^{0} and i_{corr} are the corrosion current densities values without and with inhibitor, respectively.

The electrochemical impedance spectroscopy measurements were carried out using a transfer function analyzer (VoltaLab PGZ 100), with a small amplitude *a.c.* signal (10 mV rms), over a frequency domain from 100 kHz to 100 mHz with five points per decade. The

EIS diagrams were done in the Nyquist representation. The results were then analyzed in terms of an equivalent electrical circuit using Bouckamp program [24].

The inhibiting efficiency derived from EIS, η_{EIS}, was calculated using the following Eq. (6):

$$\eta_{EIS} = \frac{R_{ct} - R_{ct}^{0}}{R_{ct}} \times 100 \quad (6)$$

Where R_{ct}^{0} and R_{ct} are the charge transfer resistance values in the absence and in the presence of inhibitor, respectively.

In order to ensure reproducibility, all experiments were repeated three times. The evaluated inaccuracy did not exceed 10%.

3. RESULTS AND DISCUSSION

3.1. Preparation and characterization of Poly(1-phenylethene)

The Poly(1-phenylethene) is synthesized by a free radical polymerization. An initiator, such as benzoyl peroxide, is used to initiate the free radical polymerization of styrene. Once the radical initiator initiates the polymerization of styrene, propagation occurs which builds up the polymer chain. Once the polymer chain has grown and at a desirable length or molecular weight, the polymerization is terminated. The polymer is then isolated, possibly purified, characterized, and used for material use. The mechanism of the free radical polymerization of styrene is shown below [25].

Formation of the radical initiator:

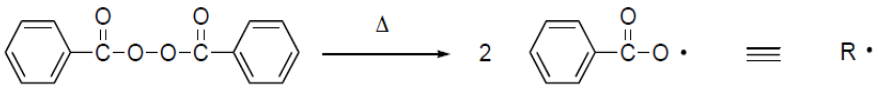

Polymerization of styrene:

Initiation:

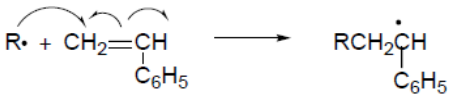

Propagation:

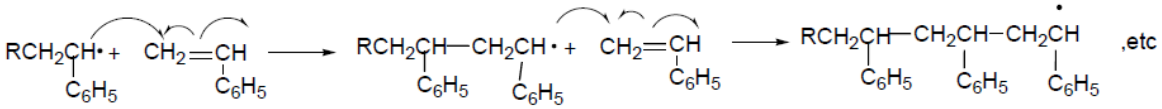

Termination:

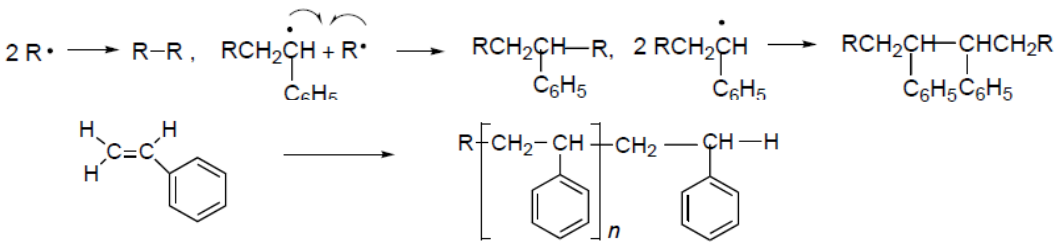

Fig. 2. Mechanism of polymerization of styrene

The FTIR spectra of Poly(1-phenylethene) was displayed in Figure 3. It is observed that the absorption peaks between 643.95 cm^{-1} and 1029.78 cm^{-1} corresponded to the benzene stretching, and bands around 1493.29 cm^{-1} for C-C units are observable. Instead, the absorption peaks at 2922.37 cm^{-1} indicated only the (asymmetric and symmetric γ of C–H units) in the spectrum of polystyrene, a strong and large absorption around 1452.82 cm^{-1} taked place in the spectrum of polystyrene corresponding to the presence of ($-CH_2$).

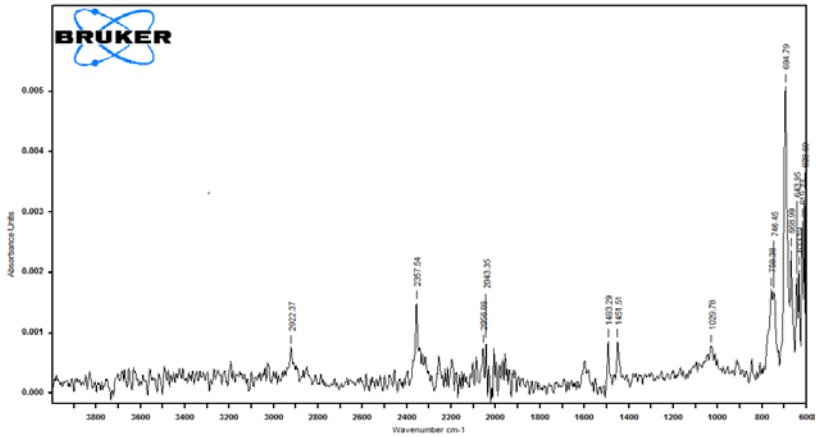

Fig. 3. FTIR spectra of Poly(1-phenylethene)

3.2. Weight loss measurements

The corrosion rate of carbon steel in 1.0 M HCl with and without different concentrations of PS was determined after 6 h of immersion at 298 K. This chose of immersion time was based according to the literature [26]. The obtained results are presented in Table 2. It has been observed that the inhibition efficiency increased with concentration of PS to reach a maximum at 200 ppm of PS. This behavior could be attributed to the increase in adsorption of inhibitor at the metal/solution interface with increasing on its concentration.

Table 2. Corrosion rate and inhibition efficiency of carbon steel in 1.0 M HCl with different concentration of PS at 298 K after 6 h of immersion

Inhibitor	*Conc. (ppm)*	ω_{corr} *(mg* cm^{-2} h^{-1}*)*	η_{ω} *(%)*	*θ*
Blank solution	**00**	**36.01**	**-**	**-**
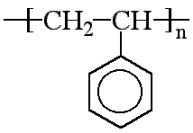	100	11.60	67.8	0.6778
	150	7.02	80.5	0.8050
	200	3.26	90.9	0.9094
	300	4.15	88.5	0.8847

So, an increase of inhibitor concentration beyond 200 ppm resulted a decreasing on corrosion

protection. This may be due to the withdrawal of adsorbate (inhibitor) back into the bulk solution when the concentration of inhibitor closed to or beyond the critical concentration. The above effect leads to the weakening of metal–inhibitor interactions, resulting in the replacement of inhibitor by water or chloride ions (Cl^-) with decrease in inhibition efficiency [21]. This may also be due to the inhibitor adsorption at the carbon steel surface through non-bonding electron pairs present on π-electrons [22].

3.3. Potentiodynamic polarization curves

Potentiodynamic polarization curves of carbon steel in 1.0 M HCl without and with different concentrations of PS at 298 K are given Figure 4 and their extrapolation parameters and inhibition efficiencies are plotted in Table 3.

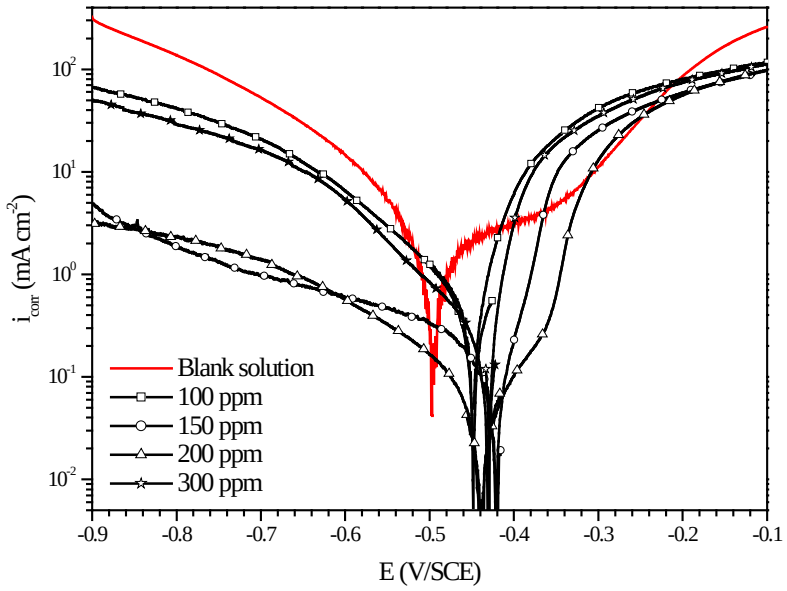

Fig. 4. Potentiodynamic polarization curves for carbon steel in 1.0 M HCl without and with different concentrations of PS

It can be seen that the PS addition hindered the acid attack on carbon steel and an increase in its concentration gave a decrease in anodic and cathodic current densities indicating that this inhibitor acted as mixed-type inhibitor. However, the inhibitor addition does not change the hydrogen evolution reaction mechanism such as indicated by the slight changes in the cathodic slopes (β_c) values. This indicated that the hydrogen evolution is activation controlled [27,28]. It is also seen that the inhibition efficiency increased with concentration to reach a maximum of 90.8% at 200 ppm of PS and exhibited both cathodic and anodic inhibition through adsorption on carbon steel surface blocking active sites [28]. So, a slight definite change on the corrosion potential (E_{corr}) was observed. According to Riggs [29] and others authors, if the displacement in E (i) is >85 mV/ E_{corr}, the inhibitor can be seen as a cathodic or anodic type, (ii) if displacement in E is <85 mV/ E_{corr}, the inhibitor can be seen as mixed

type. In our study, the maximum displacement is less than 85 mV/ E_{corr}, which indicates that PS is a mixed type inhibitor. The results obtained by the potentiodynamic polarization curves confirmed those obtained by weight loss measurements.

Table 3. Electrochemical parameters for carbon steel in 1.0 M HCl at various concentrations of PS at 298 K

Conc. of PS	$-E_{corr}$	i_{corr}	*Tafel slopes (mV dec^{-1})*		η_{PP}
(ppm)	*(mV/ SCE)*	*(μA cm^{-2})*	β_a	$-\beta_c$	*(%)*
00	497	983	203	102	-
100	429	320	63	101	67.4
150	406	231	40	103	76.5
200	443	90	62	108	90.8
300	439	112	66	105	88.6

3.4. Electrochemical Impedance Spectroscopy (EIS)

The aim of this part was to confirm the obtained results by potentiodynamic polarization curves and weight loss measurements. Figure 5 presented the Nyquist plots of carbon steel in 1.0 M HCl without and with different concentrations of PS at the corrosion potential. It can be seen that these plots were composed for one capacitive loop in the absence and presence of different concentration of PS. This behavior can be attributed to charge transfer of the corrosion process. It is also noted that the diameter of the semicircle increased with inhibitor concentration, indicating an increase in corrosion resistance of the material [30]. However, it allowed employing CPE element in order to investigate the inhibitive film properties on metallic surface. Thus, the impedance of the CPE can be described by the Eq. (7):

$$Z_{\text{CPE}} = \left[Q (j \omega)^n \right]^{-1} \quad (7)$$

Where j is the imaginary number, Q is the frequency independent real constant, $\omega=2\pi f$ is the angular frequency (rad s^{-1}), f is the frequency of the applied signal, n is the CPE exponent for whole number of n=1, 0, -1, CPE is reduced to the classical lump element-capacitor (C), resistance (R) and inductance (L) [31]. The use of these parameters, similar to the constant phase element (CPE), allowed the depressed feature of Nyquist plot to be reproduced readily.

In addition, the effective calculated double layer capacitance (C) derived from the CPE parameters according to the Eq. (8) [32]:

$$C = Q^{\frac{1}{n}} \times R^{\frac{(1-n)}{n}} \quad (8)$$

The most important data obtained from the equivalent circuit are presented in Table 4. It may be remarked that R_{ct} values increased while the C_{dl} values decreased with inhibitor

concentrations indicating that more inhibitor molecules are adsorbed on metallic surface and provided better surface coverage and/or enhanced the thickness of the protective layer at the metal/solution interface [33,34]. In addition, these change in R_{ct} and C_{dl} can be attributed to the gradual displacement of water molecules and/or chloride ions on the carbon steel surface [35], leading to a protective solid film, then a decrease in the extent of dissolution reaction [36,37]. In the other, the decrease of C_{dl} with concentration can be explained by the decrease in local dielectric constant and/or an increase in the protective layer thickness on the electrode surface. This trend is in accordance with Helmhotz model, given by the Eq. (9) [38]:

$$C_{dl} = \frac{\varepsilon_0 \times \varepsilon}{e} \times S \qquad (9)$$

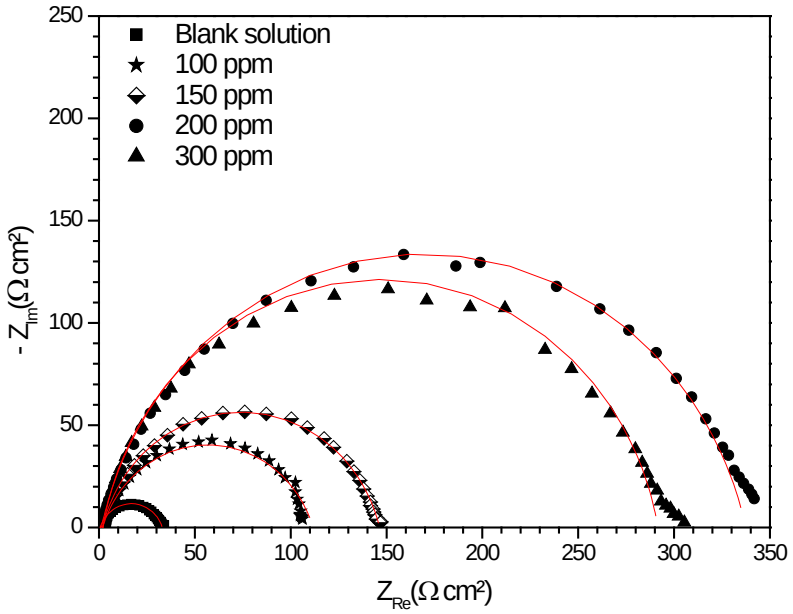

Fig. 5. Nyquist plots for carbon steel in 1.0 M HCl solution in the absence and presence of various concentrations of PS at E_{corr} (T=298 K). Scatter: Experimental curves and Red line: Fitting curves

Where ε is the dielectric constant of the protective layer, ε_0 is the permittivity of free space (8.854×10^{-14} F cm^{-1}) and S is the effective surface area of the electrode.

However, the inhibition efficiencies obtained from electrochemical impedance measurements, increase with concentration and show the same trend as those obtained from potentiodynamic polarization and gravimetric measurements.

However, the results can be interpreted using the equivalent circuit presented in Figure 6, which has been used previously to model the iron/acid interface [39]. Various parameters such as charge-transfer resistance (R_{ct}), double layer capacitance (C_{dl}) and degree of heterogeneity (n_{dl}) obtained from impedance measurements are shown in Table 4.

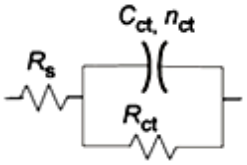

Fig. 6. Equivalent circuit used to model impedance data in 1.0 M HCl solutions in the presence of different concentration of PS

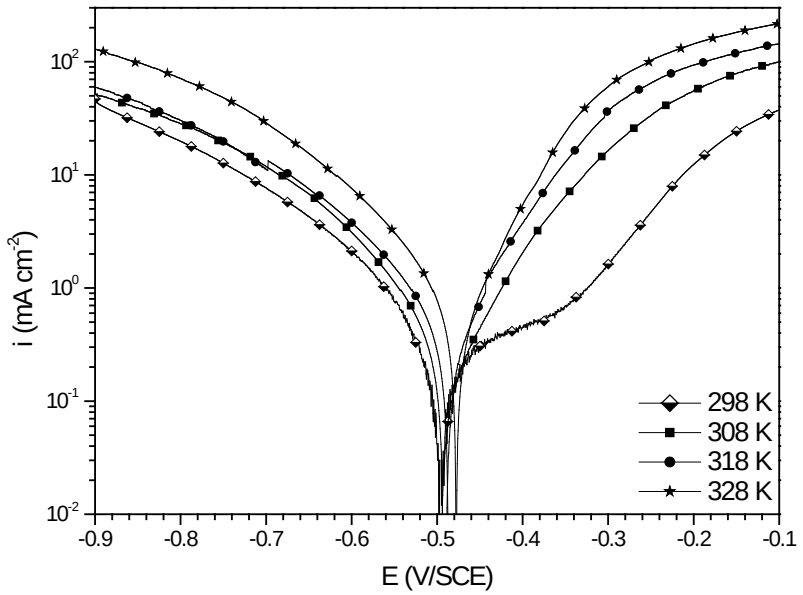

Fig. 7. Potentiodynamic polarization curves for carbon steel in 1.0 M HCl in the absence of PS at different temperature

Table 4. Electrochemical impedance parameters and inhibition efficiency for carbon steel in 1.0 M HCl solution without and with different concentration of PS at 298 K

Conc. of PS (ppm)	R_{ct} *(Ω cm^2)*	C_{dl} *(μF cm^{-2})*	n_{dl}	η_{EIS} *(%)*
00	35	284	0.79	-
100	104	240	0.80	66.3
150	149	224	0.81	77.5
200	350	95	0.85	90.0
300	305	111	0.84	89.5

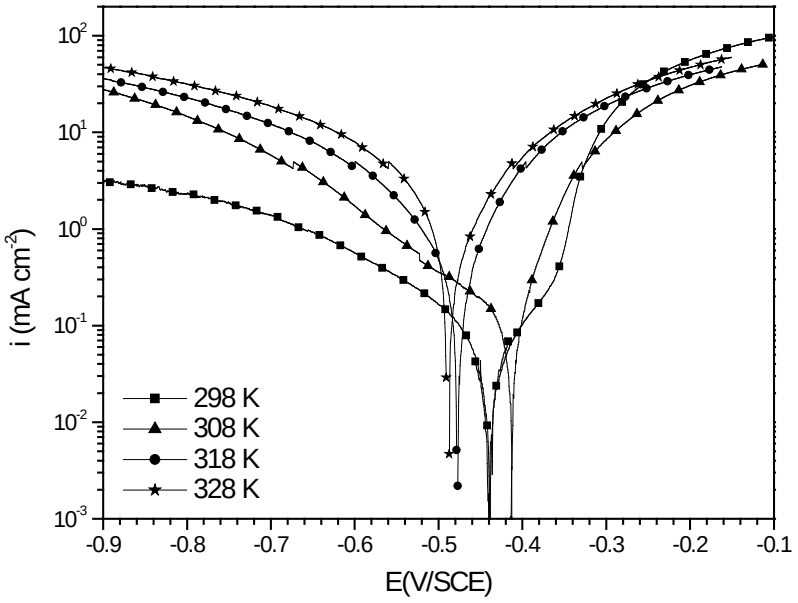

Fig. 8. Potentiodynamic polarization curves for carbon steel in 1.0 M HCl in the presence of 200 ppm of PS at different temperature

Table 5. Inhibition efficiency values obtained from weight loss, Tafel polarization and AC impedance measurements of carbon steel in 1.0 M HCl at different concentrations of PS at 298 K

Concentration of PS	***Inhibition efficiency η (%)***		
(ppm)	***Weight loss***	***Tafel polarization***	***AC impedance***
100	67.8	66.3	67.4
150	80.5	76.5	76.5
200	90.9	90.0	90.8
300	88.5	88.5	88.6

It is obvious from the results that the PS inhibited the carbon steel corrosion in 1.0 M HCl solution at its different concentrations and the η_{EIS} (%) was seen to increase continuously with the arise of concentration to reach a maximum of 92.9% at 200 ppm. The inhibition efficiencies, calculated from Tafel impedance results, showed the same trend as those obtained from EIS, polarization and weight loss measurements (Table 5).

3.5. Effect of temperature

Temperature can modify the interaction between the carbon steel electrode and the acidic media without and with PS. Thus, the potentiodynamic polarization curves for carbon steel in 1.0 M HCl in the absence and presence of 200 ppm of PS in the temperature range 298 to 328 K are shown in Figures 7 and 8 respectively. It is remarked that these curves exhibited the

Tafel regions. It is noted also that the anodic and cathodic branches increased with increasing of temperature.

The various electrochemical parameters were calculated from Tafel plots and summarized in Table 6.

It can be seen that the i_{corr} increased with increasing temperature both in uninhibited and inhibited solutions and the values of inhibition efficiency of PS decreased with increasing temperature. Thus, the inhibition efficiencies of PS are temperature-dependent.

Table 6. Electrochemical parameters of carbon steel in 1.0 M HCl without and with 200 ppm of PS at different temperature

Temperature (K)	*Blank solution*			*PS*			
	$-E_{corr}$ *(mV/SCE)*	i_{corr} *(µA/cm²)*	$-\beta_c$ *(mV/dec)*	$-E_{corr}$ *(mV/dec)*	i_{corr} *(µA/cm²)*	$-\beta_c$ *(mV/dec)*	η_{pp} *(%)*
298	498	983	92	443	90	108	91
308	491	1600	178	405	160	160	90
318	475	2420	165	470	305	145	87
328	465	3100	151	494	588	120	81

3.6. Adsorption isotherm and thermodynamic parameters

The surface coverage values (θ) of the carbon steel in 1.0 M HCl in the presence of 200 ppm of PS were obtained from the weight loss measurements (Table 2). The use of this parameter has been used to explain the best isotherm in order to determine the adsorption process. As it is known, the adsorption of an organic adsorbate onto metal/solution interface let's denote by a substitutional adsorption process between the organic molecules in the aqueous solution $PS_{(sol)}$ and the water molecules on the metallic surface $H_2O_{(ads)}$ (Eq. (10)) [29]:

$$PS_{(sol)} + X\,H_2O_{(ads)} \leftrightarrow PS_{(ads)} + XH_2O_{(ads)} \quad (10)$$

Where $PS_{(sol)}$ and $PS_{(ads)}$ are the organic molecules in the aqueous solution and adsorbed on the metallic surface, respectively, $H_2O_{(ads)}$ is the water molecules on the metallic surface, X is the size ratio representing the number of water molecules replaced by one molecule of organic adsorbate [40].

However, the Langmuir isotherm model considered was as described in reference (Eq. (11)) [41]:

$$\frac{\theta}{1-\theta} = k_{ads} \times C_{inh} \quad (11)$$

In this study, the Langmuir isotherm was fitted. The best fit straight line (strong correlation with R^2=0.9991) is obtained for the plot of C_{inh}/θ *vs*. C_{inh} with slopes around unity (Figure 9). This suggested that the adsorption of the studied inhibitor on metallic surface obeyed to the Langmuir's adsorption isotherm model, and exhibited single-layer adsorption characteristics. This kind of isotherm involved the assumption of no interaction between the adsorbed species on the electrode surface [42].

In addition, the adsorption constant, K_{ads}, was related to the free energy of adsorption, ΔG^*_{ads}, by the Eq.(12) [41]:

$$K_{ads} = \frac{1}{55.55} exp\left(\frac{-\Delta G^*_{ads}}{RT}\right) \quad (12)$$

Where 55.55 value represents the water concentration in solution by mol L^{-1}, R is the universal gas constant and T is the absolute temperature.

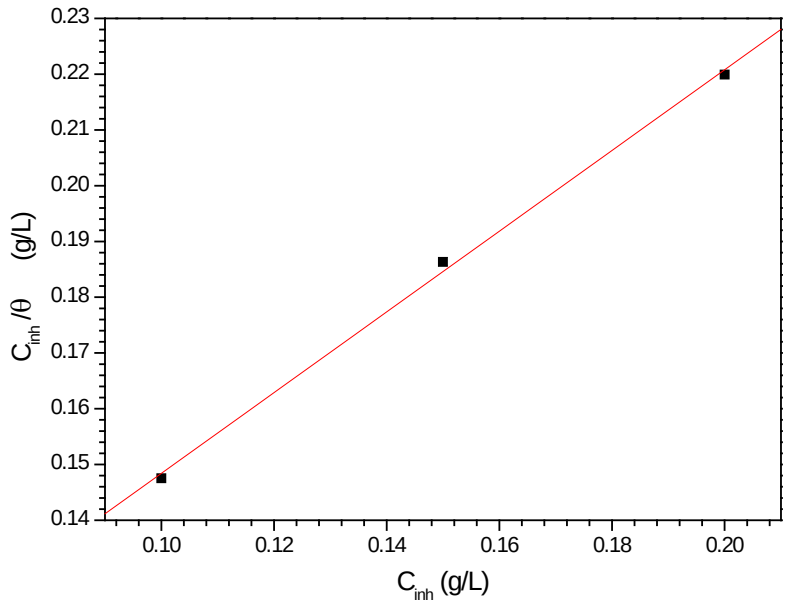

Fig. 9. Plot of the Langmuir adsorption isotherm of PS on the carbon steel surface at 298 K

The calculated value of the free energy of adsorption ΔG^*_{ads} from the adsorption isotherm is -35.71 kJ mol^{-1} at 298 K. It is well known that values of ΔG^*_{ads} of the order of -20 kJ/mol or lower indicate a physisorption, those of order of - 40 kJ/mol or higher are associated with chemisorption as a result of the sharing or transfer of electrons from organic molecules to the metal surface to form a co-ordinate, while values between -20 kJ mol^{-1} and -40 kJ mol^{-1} indicate both physisorption and chemisorption [28,33,35]. In our case, ΔG^*_{ads} values is -35.71 kJ mol^{-1} indicating that adsorption of PS occurs via both chemisorption and physisorption. In addition, the negative value of the free energy of adsorption, ΔG^*_{ads}, indicated spontaneous adsorption of organic molecules on the metallic surface and also the strong interaction between inhibitor molecules and the carbon steel surface [43,44].

3.7. Corrosion kinetic parameters

The data presented above in Table 6 revealed that the PS toke its inhibition efficiency at all temperature range. This behavior confirmed the higher adsorption equilibrium constant K_{ads} values indicating the physisorption and chemisorptions of the PS at the carbon steel surface. This result has been explained by some authors as likely specific interaction between the iron surface and the inhibitor. So, Ivanov [45] explained this increase with temperature by the change in the nature of the adsorption mode; the inhibitor is being physically adsorbed at lower temperatures, while this physisorption is favored by increasing of temperature. The same phenomenon was explained by other workers as an increase in the surface coverage by the inhibitor [46]. Thus, at a high surface coverage values, the diffusion through the surface layer containing the inhibitor and corrosion products became the rate-determining step of the metal dissolution process [47]. Thus, the inhibition properties of PS can be explained by the kinetic model. The dependence of the corrosion value i_{corr} with the temperature can be regarded as Arrhenius-type process given by Eq. (13) [48]:

$$lni_{corr} = lnA - \frac{E_a}{RT} \quad (13)$$

Where E_a is the apparent activation energy of corrosion process, R is the universal gas constant, A is the Arrhenius pre-exponential constant and T is the absolute temperature.

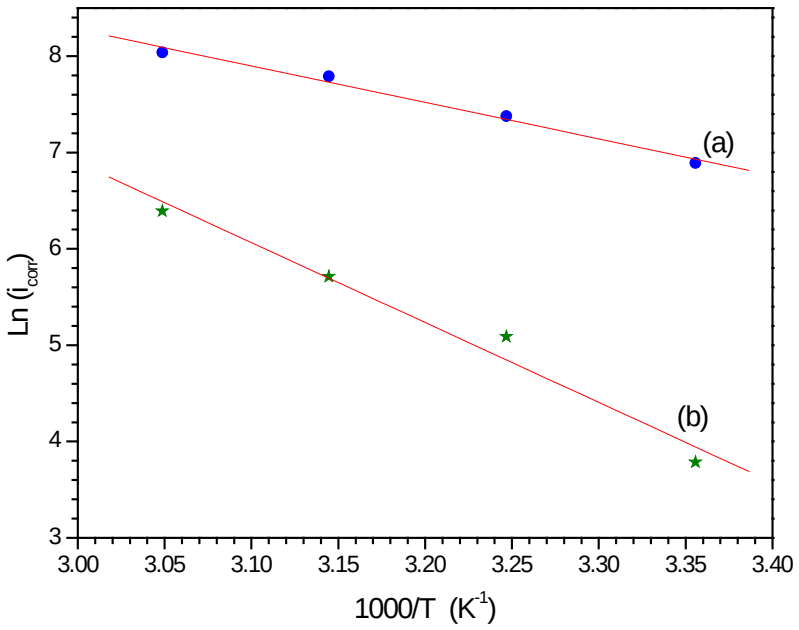

Fig. 10. Arrhenius plots of carbon steel in 1.0 M HCl (a) without and (b) with 200 ppm of PS

In order to assure that the achieved surface coverage was close to the maximal value; i.e. the concentration which gives the best inhibiting efficiency. The Arrhenius plots for carbon steel in 1.0 M HCl without and with 200 ppm of PS according to Eq. (13) were presented in Figure 10.

These plots obtained are straight lines and the slope of each straight line gives the activation energy value E_a. It is noted that the increase of corrosion rate is more pronounced with the rise of temperature for free solution. So, in the presence of PS, the corrosion rate is slightly increased at explores temperatures. The E_a values were found to be equal to 31.5 kJ mol^{-1} and 69 KJ mol^{-1} in the absence and presence of 200 ppm of PS (Table 7).

The decrease of the inhibitor efficiency with increasing temperature, which referred to a higher value of E_a, when compared to free solution, was interpreted as an indication for an electrostatic character of the inhibitor's adsorption. So, the investigated inhibitor blocked significantly some of the active sites on the metal surface inhomogeneous energetically. In general, the inhibitor adsorbed at the most active sites of the surface with lowest E_a and thus isolated them. Other active sites of higher E_a take part in the further corrosion process.

In addition, this change in E_a with PS addition can be attributed to the change in the corrosion process mechanism in the presence of adsorbed inhibitor molecules [49].

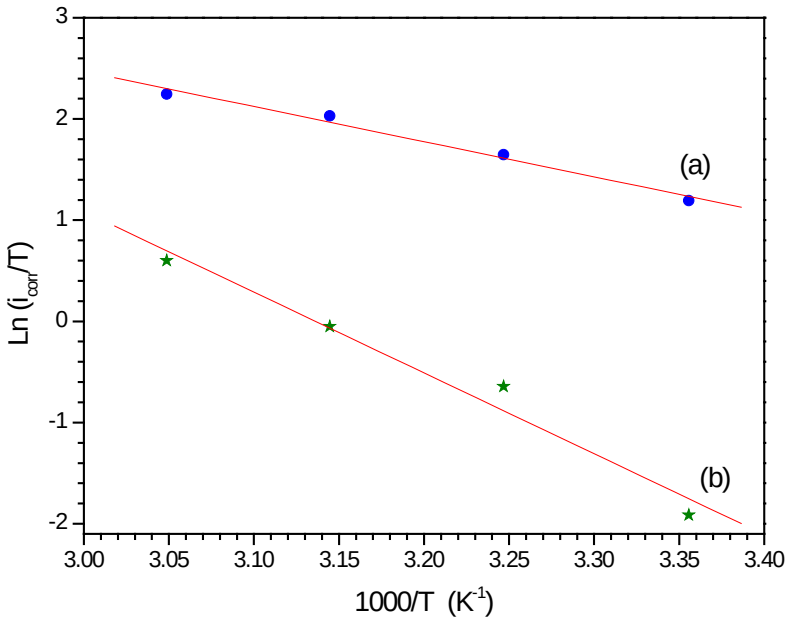

Fig. 9. Transition-state plots for carbon steel in 1.0 M HCl (a) without and (b) with 200 ppm of PS

Other kinetic data are accessible using the alternative formulation of the Arrhenius Equation is (Eq. (14)) [51]:

$$ln\frac{i_{corr}}{T} = \left(ln\left(\frac{R}{Nh}\right) + \frac{\Delta S_a^*}{R}\right) - \frac{\Delta H_a^*}{RT} \qquad (14)$$

Where h is Plank's constant, N is Avogadro's number, ΔS_a^* is the entropy of activation and ΔH_a^* is the enthalpy of activation.

Plots of Ln (i_{corr}/T) versus the reciprocal of temperature (1/T) of carbon steel in 1.0 M HCl without and with 200 ppm of PS are presented in Figure 11. Straight lines are obtained with a slope of (-ΔH_a*/R) and an intercept of (lnR/Nh+ΔS_a^*/R). The values of ΔH_a^* and ΔS_a^* are calculated and are listed in Table 7. The positive sign of the enthalpies ΔH_a^* improved the endothermic nature of the carbon steel dissolution process whereas large negative values of entropies ΔS_a^* implied that the activated complex in the rate determining step represents an association rather than a dissociation step, meaning that a decrease in disordering takes place on going from reactants to the activated complex [51,49-53].

Table 7. The values of activation parameters E_a, ΔH_a^* and ΔS_a^* for carbon steel in 1.0 M HCl in the absence and presence of 200 ppm of PS

Compounds	***E_a (kJ mol^{-1})***	***ΔH_a^* (kJ mol^{-1})***	***ΔS_a^* (J mol^{-1} K^{-1})***
Blank solution	31.5	28	-107
PS	69	64	-164

4. CONCLUSION

Concluding the experimental part, it was clearly demonstrated that all techniques used, are able to characterize and to follow the corrosion inhibition process promoted by poly(1-phenylethene). The following conclusions can be drawn:

The corrosion rate of carbon steel decreased with increasing the inhibitor concentration to reach a minimum at 200 ppm. Poly(1-phenylethene) exhibited good inhibition properties for carbon steel corrosion in 1.0 M HCl solution and increased with increasing the concentration of inhibitor. The obtained results showed that PS acted as mixed-type inhibitor of carbon steel corrosion in 1.0 M HCl.

EIS measurement results indicated that the resistance of the carbon steel electrode increased with inhibitor concentrations to reach a maximum at 200 ppm of PS. The inhibition efficiency of PS can be stabilized by the participation of the tow adsorption mode, physisorption and chemisorptions. Thermodynamic adsorption parameters (ΔH_a^*, ΔS_a^* and ΔG_a^*) showed that the studied inhibitor was adsorbed on carbon steel surface by an endothermic and spontaneous process. Reasonably good agreement was observed between the obtained data from weight loss, potentiodynamic polarization curves and electrochemical impedance spectroscopy techniques.

REFERENCES

[1] Y. El Kacimi, R. Touir, M. Galai, R. A. Belakhmima, A. Zarrouk, K. Alaoui, M. Harcharras, H. El Kafssaoui, and M. Ebn Touhami, J. Mater. Environ. Sci. 7 (2016) 371.

[2] M. HazwanHussin, M. Jain Kassim, N. N. Razali, N. H. Dahon, and D. Nasshorudin, Arabian J. Chem. (2011)1878.
[3] Y. Abbouda, A. Abourriche, T. Saffaj, M. Berrada, M. Charrouf, A. Bennamara, N. Al Himidi, and H. Hannache, Mater. Chem. Phys.105 (2007) 1.
[4] A. O. James, N. C. Oforka, and K. Abiola, Int. J. Electrochem. Sci. 2 (2007) 284.
[5] E. E. Ebenso, Niger. J. Chem. Res. 6 (2001) 12.
[6] U. J. Ekpe, P. C. Okafor, E. E. Ebenso, O. E. Offiong, and B. I. Ita, Bull. Electrochem.17 (2001) 135.
[7] Y. Elkacimi, M. Achnin, Y. Aouine, M. Ebn Touhami, A.Alami, R. Touir, M. Sfaira, D. Chebabe, A. Elachqar, and B. Hammouti, Portugaliae Electrochim. Acta 30 (2012) 53.
[8] E. A. Noor, and A. H. Al-Moubaraki, Int. J. Electrochem. Sci. 3 (2008) 806.
[9] Esmaeel Naderi, A. H. Jafari, M. Ehteshamzadeh, and M. G. Hosseini, Mater. Chem. Phys. 115 (2009) 852.
[10] F. Bentiss, M. Lagrenee, M. Traisnel, and J. C. Hornez, Corros. Sci. 41 (1999) 789.
[11] M. Ozcan, and I. Dehri, Prog. Org. Coat. 51 (2004) 181.
[12] M. Ehteshamzade, T. Shahrabi, and M. G. Hosseini, Appl. Surf. Sci. 252 (2006) 2949.
[13] M. Lebrini, F. Bentiss, H. Vezin, and M. Lagren´ee, Corros. Sci. 48 (2006) 1279.
[14] H. Bhandari, R. Srivastav, V. Choudhary, and S. K. Dhawan, Thin Solid Films 519 (2010) 1031
[15] S. K. Shukla, M. A. Quraishi, and R. Prakash, Corros. Sci. 50 (2008) 2867
[16] Y. Ren, Y. Luo, K. Zhang, G. Zhu, and X. Tan, Corros. Sci. 50 (2008) 3147
[17] G. Achary, Y. A. Naik, S. V. Kumar, T. V. Venkatesha, and B. S. Sherigara, Appl. Surf. Sci. 254 (2008) 5569.
[18] M. M. Solomon, S. A. Umoren, I. I. Udosoro, and A. P. Udoh, Corros. Sci. 52 (2010) 1317.
[19] S. K. Shukla, M. A. Quraishi, J. Appl. Polym. Sci. 124 (2012) 5130
[20] K. Alaoui, Y. El Kacimi, M. Galai, R. Touir, K. Dahmani, A. Harfi, and M. Ebn Touhami, J. Mater. Environ. Sci. 7 (2016) 2389.
[21] ASTM G-81., Annual Book of ASTM Standards, (1995).
[22] M. Stern, and A. L. Geary, J. Electrochem. Soc. 104 (1957) 56.
[23] M. S. AbdelAal, S. Radwan, and A. El Saied, Br. Corros. J. 18 (1983) 2.
[24] K. L. Williamson, and R. D. Minard, K. M. Masters Macroscale and Microscale Organic Experiments, 5th Ed. Hougton Miffilin Co.; Boston (2007) pp 774.
[25] D. B.Hmamou, R. Salghi, A. Zarrouk, M. R. Aouad, O. Benali, H. Zarrok, M. Messali, B. Hammouti, M. Kabanda, M. Bouachrine, and E. E. Ebenso. Ind. Eng. Chem. Res. 52 (2013) 14315.
[26] B. G. Ateya, M. B. A. El-Khair, and I. A. Abdel-Hamed, Corros. Sci. 16 (1976)163.
[27] W. Li, Q. He, S. Zhang, C. Pei, and B. Hou, J. Appl. Electrochem. 38 (2008) 289.

[28] M. A. Quraishi, S. Ahmad, and G. Venkatachari, Bull. Electrochem. 12 (1996) 109.
[29] O. L. Riggs, Jr, in C. C. Nathan (Ed), Corrosion Inhibition, NACE, Houston, TX, (1973) pp 11.
[30] S. Ghareba, and S. Omanovic, Corros. Sci. 52 (2010) 2104.
[31] H. Gerengi, K. Darowicki, G. Bereket, and P. Slepski, Corros. Sci. 51 (2009) 2573.
[32] G. J. Brug, A. L. G.Van DenEeden, M. Sluyters-Rehbach, and J. H. Sluyters, J. Electroanal. Chem. 176 (1984) 275.
[33] M. Moradi, J. Duan, and X. Du, Corros. Sci. 69 (2013) 338.
[34] Y. Tang, F. Zhang, S. Huc, Z. Cao, Z. Wu, and W. Jing, Corros. Sci.74 (2013) 271.
[35] J. W. Schultze, and K. Wippermann, Electrochim. Acta 32 (1987) 823.
[36] S. Martinez, M. Metikos, and Hukovic, J. Appl. Electrochem. 33 (2003) 137.
[37] C. H. Hsu, and F. Mansfeld, Corrosion 57 (2001) 747.
[38] E. Khamis, Corrosion 46 (1990) 6.
[39] F. Bentiss, M. Lebrini, and M. Lagrene´e, Corros. Sci. 47 (2005) 2915.
[40] K. Adardour, O. Kassou, R. Touir, M. Ebn Touhami, H. El Kafsaoui, H. Benzeid, M. Essassi, and M. Sfaira, J. Mater. Environ. Sci. 1 (2010) 129.
[41] K. F. Khaled, Electrochim. Acta 53 (2008) 3484.
[42] A. Srhiri, M. Etman, and F. Dabosi, Werkst. Korros.43 (1992) 406.
[43] M. Elayyachy, A. El Idrissi, and B. Hammouti, Corros. Sci. 48 (2006) 2470.
[44] F. Hongbo, Synthesis and application of new type inhibitors, Chemical Industry Press, Beijing, (2002) pp. 166.
[45] S. A. Ali, H. A. Al-Muallem, M. T. Saeed, and S. U. Rahman, Corros. Sci. 50 (2008) 664.
[46] A. Popova, Corros. Sci. 49 (2007) 2144.
[47] I. Putilova, S. Balezine, and V. Barannik, in Metalic Corrosion Inhibitors, Ed. by E. Bishop, London, England, (1960).
[48] R. Raicheff, K. Valcheva, and E. Lazarova, in: Proceeding of the Seventh European Symposium on Corrosion Inhibitors, Ferrara, Italy (1990) 48.
[49] L. Herrag, B. Hammouti, S. Elkadiri, A. Aouniti, C. Jama, H. Vezin, and F. Bentiss, Corros. Sci. 52 (2010) 3042.
[50] J. Marsh, Advanced Organic Chemistry, 3rd edn. Wiley Eastern, New Delhi, (1988).
[51] S. Martinez, and I. Stern, Appl. Surf. Sci. 199 (2002) 83.
[52] M. Dahmani, A. Et-Touhami, S. S. Al-Deyab, B. Hammouti, A. Bouyanzer, Int. J. Electrochem. Sci. 5 (2010) 1060.